Available online at www.sciencedirect.com
ScienceDirect
Surface Science 601 (2007) 865–870
SURFACE SCIENCE
www.elsevier.com/locate/susc

Angular and energy dependences of the surface excitation parameter for semiconducting III–V compounds

Y.H. Tu [a], C.M. Kwei [a], C.J. Tung [b,*]

[a] Department of Electronics Engineering, National Chiao Tung University, Hsinchu 300, Taiwan
[b] Department of Nuclear Science, National Tsing Hua University, Hsinchu 300, Taiwan

Received 27 April 2006; accepted for publication 14 November 2006
Available online 4 December 2006

Abstract

Sum-rule-constrained extended Drude dielectric functions were used to study surface excitations generated by energetic electrons moving across surfaces of semiconducting III–V compounds. Parameters in the dielectric functions were determined from fits to experimental optical data and electron energy-loss spectra. Electron inelastic mean free paths (IMFPs) in GaN, GaP, GaAs, GaSb, InAs and InSb were calculated for electron energies between 200 and 2000 eV, and the results were found to follow the simple formula, i.e., $\lambda = kE^p$, where λ is the IMFP and E is the electron energy. Surface excitation parameters (SEPs), which describe the total probability of surface excitations by electrons crossing the surface and travelling in vacuum, were also calculated for different electron energies and crossing angles. The SEP was found to follow the simple formula, i.e., $P_s = \frac{aE^{-b}}{\cos^c \alpha}$, where P_s is the SEP and α is the crossing angle relative to the surface normal.

Keywords: Electron; Dielectric function; Inelastic mean free path; Surface excitation parameter

1. Introduction

Quantitative information on the inelastic interactions between electrons and solids is important in surface-sensitive spectroscopies such as Auger electron spectroscopy (AES), X-ray photoelectron spectroscopy (XPS) and reflection electron energy-loss spectroscopy (REELS). Recent studies on the energy-loss spectra [1–3] of electrons reflected from solid surfaces have demonstrated that the contribution from surface excitations was important for electron energies from a few hundred eV to several keV, especially with obliquely incident or escaping electrons. Therefore, surface excitations should be included in the analyses of electron spectroscopies.

Many theoretical approaches [4–11] have been proposed to deal with the surface excitations in inelastic interactions. Such excitations were most conveniently characterized by the so-called surface excitation parameter (SEP), defined as the average number of surface excitations by an electron crossing the solid surface [12,13]. For an electron moving inside the solid, the decrease in surface excitations as the electron moves away from the surface is nearly compensated by the increase in volume excitations. It is therefore more convenient to treat surface and volume excitations together in the solid. Because of this, Kwei et al. [13] calculated the SEP by integrating the inverse inelastic mean free path (IMFP) for an electron, either incident or escaping, moving only in vacuum. These calculations were made primarily for normally incident and escaping electrons. For other tilted crossing angles, α, the SEP was approximated by multiplying the SEP for a normally crossing angle by $(\cos\alpha)^{-1}$ [13,14]. Such calculations, however, only approximately satisfied the conservations of energy and momentum due to the use of cylindrical coordinates that carried no restriction on the normal component of momentum transfer [15,16]. Later, Werner et al. [17–19] rescaled the

* Corresponding author. Tel./fax: +886 3 5727300.
E-mail address: cjtung@mx.nthu.edu.tw (C.J. Tung).

0039-6028/$ - see front matter © 2006 Elsevier B.V. All rights reserved.
doi:10.1016/j.susc.2006.11.020

electron momentum in Oswald's free-electron theory [20] by material-dependent parameters to estimate the SEP for an arbitrary material. They listed these parameters for some materials [18], but did not include semiconducting III–V compounds.

Recently, Li et al. [15,16] developed a model for the SEP with arbitrary crossing angles. The model employed spherical coordinates for the momentum transfer and thus satisfied the conservations of energy and momentum. In the present work, this model was applied using extended Drude dielectric functions with spatial dispersion [21] for semiconducting III–V compounds. Fitting parameters in the dielectric functions were determined from experimental data [22–25], a combination of optical data and electron energy-loss spectra, and checked using sum rules and characteristic energies for the interband transitions and plasma excitations. These dielectric functions were then applied to calculate the IMFPs and SEPs for semiconducting III–V compounds. The dependences of the SEP on electron energy and crossing angle are analyzed, and compared with other theoretical results and measured data.

2. Methods

The extended Drude dielectric function is given by [21]

$$\varepsilon(q,\omega) = \varepsilon_1(q,\omega) + i\varepsilon_2(q,\omega) = \varepsilon_B - \sum_i \frac{A_i}{\omega^2 - \left(\omega_i + \frac{q^2}{2}\right)^2 + i\omega\gamma_i}, \quad (1)$$

where A_i, γ_i and ω_i are, respectively, the oscillator strength, damping coefficient and resonant frequency, all associated with the ith group of electrons in the valence band and, sometimes, the outermost inner shells. The background dielectric function, ε_B, is included in Eq. (1) to account for the influence of polarizable ion cores [26]. In the present work, we fit $\varepsilon_2(0,\omega)$ and $\mathrm{Im}[-1/\varepsilon(0,\omega)]$ using Eq. (1) to experimental optical data [22,23] and electron energy-loss spectra [24,25] to determine the parameters A_i, γ_i, ω_i, and ε_B. Table 1 gives the sources of optical data and electron energy-loss spectra. Since small differences in ε_1 and ε_2 around the valence plasmon peak could generate a large difference in $\mathrm{Im}(-1/\varepsilon)$, data on the energy-loss function derived directly from measured electron energy-loss spectra are used, if available, for energy transfers in the vacuum ultraviolet spectral region. At smaller energy transfers, i.e., in the infrared spectra region, optical data are, instead, used because they provide detailed information on the interband transitions with reasonable accuracy. Here we make use of optical data determined using the ellipsometry, a powerful method in determining ε_1 and ε_2 without resorting to the Kramers–Kronig analysis. Since optical data are usually available regarding the extinction coefficient and the refractive index in limited frequency ranges, extrapolations are sometimes required [27–29]. In the present fits, we also require $\varepsilon_1(0,\omega)$ and $\mathrm{Im}\{-1/[\varepsilon(0,\omega)+1]\}$ to be in good agreement with experimental data. Detailed inspection of experimental $\mathrm{Im}(-1/\varepsilon)$ data shows that the energy-loss function extends over sufficiently wide energy transfers. This is due to the strong overlapping of oscillator strengths between electrons in the valence band and the outermost inner shells. The present fits include the contribution from all such electrons.

Table 1
Sources of optical data and energy-loss spectra

Material	Photon-energy range (eV)	Sources
GaN	<27	Ref. [25]
GaP	<6	Ref. [22]
	6–25	Ref. [24]
	25–154	Ref. [22] and extrapolation
GaAs	<6	Ref. [22]
	6–25	Ref. [24]
	25–155	Ref. [22] and extrapolation
GaSb	<6	Ref. [23]
	6–25	Ref. [24]
InAs	<6	Ref. [22]
	6–25	Ref. [24]
InSb	<6	Ref. [22]
	6–25	Ref. [24]
	25–155	Ref. [22] and extrapolation

To assure the accuracy of the dielectric function fittings, we check the validities of the sum rules

$$\int_0^\omega \omega'\varepsilon_2(0,\omega')\mathrm{d}\omega' = 2\pi^2 NZ(\omega) \quad (2)$$

and

$$\int_0^\omega \omega'\mathrm{Im}\left[\frac{-1}{\varepsilon(0,\omega')}\right]\mathrm{d}\omega' = 2\pi^2 N\frac{Z'(\omega)}{\varepsilon_B^2}, \quad (3)$$

where N is the molecular density and $Z(\omega)$ and $Z'(\omega)$ are the corresponding effective numbers of electrons per molecule by excitations up to the energy transfer ω. At small ω, only valence electrons contribute to $Z(\omega)$ and $Z'(\omega)$. As ω increases to a value close to the binding energy of the outermost inner-shell, inner-shell electrons begin to contribute. When ω goes to infinity, both $Z(\omega)$ and $Z'(\omega)$ should saturate to Z_m, the total number of electrons per molecule. However, optical data usually cover the ω region with contributions only from the valence band and the outermost inner shell. Thus Z_m is unattainable from the integration of Eq. (2) or (3) using either the optical data or the fit results to these data. In practice, sum rules can be applied by setting the upper limits of integration in Eqs. (2) and (3) to finite and infinite values. In the case of finite-range sum rules, we compare $Z(\omega)$ and $Z'(\omega)$ between results calculated from the present fits and using the optical data at any given ω below the maximum available energy transfer in the optical data. The accuracy of these comparisons varies from material to material and depends on the value of ω. In general, fitting values are adopted with an overall accuracy of a few percent. For the application of infinite-range sum rules, we check $\sum_i A_i = 4\pi NZ'_m$ to verify if Z'_m includes the contribution from the valence band and the outermost inner shell.

For an electron traveling in a homogeneous, isotropic and infinite solid, the inverse IMFP is given by [30,31]

$$\lambda^{-1}(E) = \frac{1}{\pi E}\int_0^E \mathrm{d}\omega \int_{q_-}^{q_+} \frac{\mathrm{d}q}{q}\,\mathrm{Im}\left[\frac{-1}{\varepsilon(q,\omega)}\right], \tag{4}$$

where E is the electron energy and $q_\pm = \sqrt{2E} \pm \sqrt{2(E-\omega)}$ are derived from conservations of energy and momentum. Note that atomic units (a.u.) are used throughout unless otherwise specified.

The SEP is defined as the integration of the inverse IMFP for an electron, either incident or escaping, moving in vacuum. For obliquely escaping (from solid to vacuum: s → v) and incident (from vacuum to solid: v → s) electrons, the SEP may be given in the dielectric response theory as [15]

$$\begin{aligned} P_{\mathrm{s}}^{\mathrm{s}\to\mathrm{v}}(\alpha,E) = {} & \frac{4\cos\alpha}{\pi^3}\int_{-\infty}^{0}\mathrm{d}r\int_0^E \mathrm{d}\omega\int_{q_-}^{q_+}\mathrm{d}q \\ & \times \int_0^{\pi/2}\mathrm{d}\theta\int_0^{2\pi}\mathrm{d}\phi\left[2\cos\left(\frac{\tilde{\omega}r}{v}\right) - \exp(-|r|Q\cos\alpha)\right] \\ & \times \frac{q\sin^2\theta\exp(-|r|Q\cos\alpha)}{\tilde{\omega}^2+Q^2v_\perp^2}\,\mathrm{Im}\left[\frac{-1}{\varepsilon(q,\omega)+1}\right] \end{aligned} \tag{5}$$

and

$$\begin{aligned} P_{\mathrm{s}}^{\mathrm{v}\to\mathrm{s}}(\alpha,E) = {} & \frac{4\cos\alpha}{\pi^3}\int_{-\infty}^{0}\mathrm{d}r\int_0^E \mathrm{d}\omega\int_{q_-}^{q_+}\mathrm{d}q \\ & \times \int_0^{\pi/2}\mathrm{d}\theta\int_0^{2\pi}\mathrm{d}\phi\,\frac{q\sin^2\theta\cos(q_z r\cos\alpha)}{\tilde{\omega}^2+Q^2v_\perp^2} \\ & \times \exp(-|r|Q\cos\alpha)\,\mathrm{Im}\left[\frac{-1}{\varepsilon(q,\omega)+1}\right], \end{aligned} \tag{6}$$

where $Q = q\sin\theta$, $q_z = q\cos\theta$, $v_\perp = \sqrt{2E}\cos\alpha$ and $\tilde{\omega} = \omega - qv\sin\theta\cos\phi\sin\alpha$. The crossing angle α is defined as the angle between the surface normal and the electron direction. Eqs. (5) and (6) indicate that the SEP depends on electron energy and crossing angle. Its value is different for incident and escaping electrons.

3. Results and discussion

Table 2 lists the fit parameters in Eq. (1) for the semiconducting III–V compounds, GaN, GaP, GaAs, GaSb, InAs and InSb. A comparison between the present fits (solid curves) and experimental data [25] (dotted curves) for $\varepsilon_1(0,\omega)$, $\varepsilon_2(0,\omega)$, $\mathrm{Im}[-1/\varepsilon(0,\omega)]$ and $\mathrm{Im}[-1/(\varepsilon(0,\omega)+1)]$ is shown in Fig. 1 for GaN. It is seen that the fits are in good agreement with experimental data.

IMFPs for electrons moving in semiconducting III–V compounds can be calculated using Eq. (4) and the fit parameters in Table 2. An analysis of the calculated results yields a relation for the IMFP as

$$\lambda(E) = kE^p, \tag{7}$$

Table 2
Parameters in Eq. (1) for semiconducting III–V compounds

GaN ($\varepsilon_B = 1.35$)		GaP ($\varepsilon_B = 1.05$)		GaAs ($\varepsilon_B = 1.01$)		GaSb ($\varepsilon_B = 1.02$)		InAs ($\varepsilon_B = 1.05$)		InSb ($\varepsilon_B = 1.02$)	
A_i(eV^2)	γ_i(eV)	A_i(eV^2)	γ_i(eV)	A_i(eV^2)	γ_i(eV)	A_i(eV^2)	γ_i(eV)	A_i(eV^2)	γ_i(eV)	A_i(eV^2)	γ_i(eV)
3.90	0.90	3.40	2.00	2.08	0.10	3.40	0.20	2.30	0.20	6.00	0.34
87.00	2.20	12.50	0.20	25.97	0.61	23.70	0.68	22.50	0.76	21.50	0.77
33.00	6.00	34.00	0.90	31.90	1.20	38.90	1.15	85.00	2.60	42.00	1.50
25.00	1.60	40.90	0.80	58.80	0.70	28.70	0.70	28.70	0.46	34.70	0.68
56.00	3.00	58.70	0.70	17.00	0.35	27.00	0.48	5.00	0.90	5.00	0.90
13.00	3.00	10.00	2.00	10.00	1.00	7.50	0.80	4.00	0.60	7.00	2.00
28.00	1.80	40.00	1.70	43.44	2.42	8.00	0.70	5.00	0.60	16.00	1.20
79.00	2.50	45.00	4.00	48.00	10.30	5.00	0.80	8.00	2.00	8.00	1.20
33.00	3.00	15.00	5.00	5.60	2.80	15.00	1.80	45.00	5.90	20.00	3.30
30.00	3.00	3.00	3.00	1.50	2.00	28.00	3.00	10.00	5.50	4.20	7.50
49.00	4.40	4.50	3.00	5.00	3.20	3.50	2.50	23.00	5.00	3.60	3.00
1.20	3.20	16.00	25.20	15.00	29.30	1.30	1.50	30.00	35.00	6.00	2.50
3.60	1.80	19.00	29.40	25.00	36.70	10.10	5.50	40.00	36.80	5.00	3.00
23.00	2.00	102.00	39.00	40.00	38.20	1.80	1.50			2.00	2.00
12.00	3.00					1.20	1.50			3.00	2.00
160.00	4.10					6.50	3.60			10.00	29.60
						30.00	30.00			16.00	33.00
						40.00	35.00			130.00	35.00
						50.00	38.00				

GaN ($\varepsilon_B = 1.35$)		GaP ($\varepsilon_B = 1.05$)		GaAs ($\varepsilon_B = 1.01$)		GaSb ($\varepsilon_B = 1.02$)		InAs ($\varepsilon_B = 1.05$)		InSb ($\varepsilon_B = 1.02$)	
A_i(eV^2)	ω_i(eV)	A_i(eV^2)	ω_i(eV)	A_i(eV^2)	ω_i(eV)	A_i(eV^2)	ω_i(eV)	A_i(eV^2)	ω_i(eV)	A_i(eV^2)	ω_i(eV)
3.90	3.98	3.40	2.00	2.08	2.89	3.40	2.10	2.30	2.50	6.00	1.89
87.00	6.98	12.50	0.20	25.97	3.73	23.70	2.50	22.50	2.80	21.50	2.40
33.00	7.00	34.00	0.90	31.90	4.02	38.90	3.30	85.00	4.15	42.00	3.35
25.00	8.70	40.90	0.80	58.80	4.80	28.70	3.80	28.70	4.48	34.70	3.85
56.00	9.80	58.70	0.70	17.00	5.10	27.00	4.11	5.00	4.85	5.00	4.18
13.00	10.50	10.00	2.00	10.00	5.45	7.50	4.80	4.00	5.40	7.00	4.53
28.00	11.20	40.00	1.70	43.44	6.80	8.00	5.20	5.00	6.10	16.00	5.23
79.00	12.80	45.00	4.00	48.00	9.80	5.00	5.80	8.00	6.90	8.00	5.96
33.00	13.20	15.00	5.00	5.60	13.20	15.00	7.00	45.00	8.80	20.00	8.50
30.00	14.80	3.00	3.00	1.50	22.00	28.00	8.50	10.00	19.50	4.20	9.50
49.00	17.30	4.50	3.00	5.00	24.00	3.50	10.50	23.00	23.00	3.60	10.20
1.20	19.90	16.00	25.20	15.00	26.00	1.30	11.20	30.00	32.00	6.00	19.80
3.60	21.30	19.00	29.40	25.00	30.00	10.10	12.00	40.00	38.00	5.00	21.00
23.00	22.80	102.00	39.00	40.00	40.00	1.80	20.20			2.00	23.50
12.00	25.00					1.20	21.30			3.00	24.50
160.00	29.00					6.50	24.00			10.00	30.00
						30.00	31.00			16.00	34.00
						40.00	36.00			130.00	36.00
						50.00	40.00				

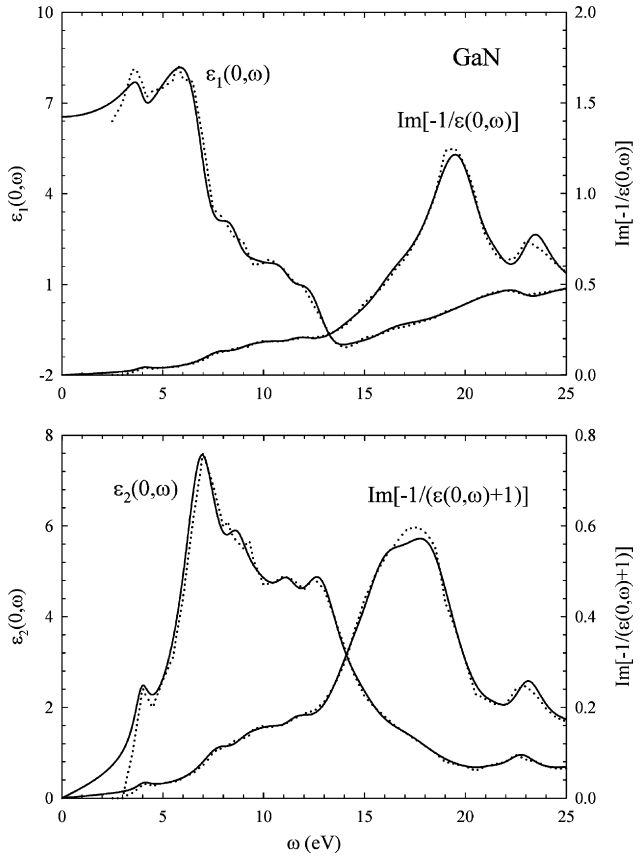

Fig. 1. A plot of the real and imaginary parts of the dielectric function, $\varepsilon_1(0,\omega)$ and $\varepsilon_2(0,\omega)$, the volume loss function, $\mathrm{Im}[-1/\varepsilon(0,\omega)]$, and the surface loss function, $\mathrm{Im}[-1/(\varepsilon(0,\omega)+1)]$, for GaN. Solid and dotted curves are, respectively, results of fits made with Eq. (1) and experimental data [25].

where k and p are adjustable parameters. With λ in angstroms and E in electron-volts, the best-fitted values of k and p are listed in Table 3 for electron energies from 200 to 2000 eV. These values are somewhat different from those obtained previously [32]. The differences are due to the inclusion here of the contribution of polarized ion cores and inner-shells. Fig. 2 shows the IMFPs for InAs. The solid circles, solid curve and open circles are, respectively, the calculated results using Eq. (4), the fitted data using Eq. (7), and the experimental data measured by Gergely et al. [33]. The corresponding results from the Tanuma et al. [34] calculations (dashed curve) and the Gries [35] predictive equation (dotted curve) are included for comparison. It is seen that the fitted data are in excellent agreement with the other results.

Table 3
Parameters in Eq. (7) for semiconducting III–V compounds

Material	k	p
GaN	0.1231	0.7980
GaP	0.0896	0.8125
GaAs	0.0877	0.8160
GaSb	0.0888	0.8196
InAs	0.0957	0.8174
InSb	0.0910	0.8207

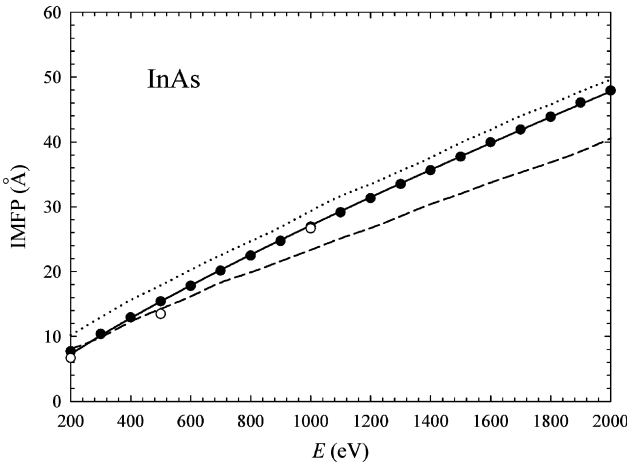

Fig. 2. A plot of electron IMFP in InAs as a function of electron energy. Solid circles and solid curve are results calculated using Eq. (4) and fitted using Eq. (7). Open circles are experimental data measured by Gergely et al. [33]. Dashed and dotted curves are results calculated by Tanuma et al. [34] and Gries [35], respectively.

The SEPs for semiconducting III–V compounds were calculated for both escaping and incident electrons using Eqs. (5) and (6). The calculated results were found to follow the simple formula

$$P_s^{s\to v}(\alpha,E) \quad \text{or} \quad P_s^{v\to s}(\alpha,E)=\frac{aE^{-b}}{\cos^c\alpha}, \tag{8}$$

where a, b and c are material-dependent coefficients. With E in electron-volts, the best-fit values of parameters a, b and c are listed in Table 4. These values are different from those found previously for $\alpha=0°$ [36], where the laws of conservation of energy and momentum were not completely satisfied [15,16]. Fig. 3 shows a plot of the SEP as a function of crossing angle for 800 eV electrons moving from vacuum to GaSb. The solid circles, solid curve and dashed curve are, respectively, calculated results using Eq. (6), fitted data of the present work using Eq. (8), and results of the previous work [36]. Fig. 3 shows that the assumption of the angular dependence of SEP in the previous work, $(\cos\alpha)^{-1}$, is valid only approximately. We now find that the SEP is greater for larger crossing angles due to the longer interaction time between the electron and the surface. The SEP rises slowly with increasing crossing angle until about $\alpha=70°$, an appreciable glancing angle, above which it increases rapidly.

Table 4
Parameters in Eq. (8) for semiconducting III–V compounds

Material	Escaping electrons			Incident electrons		
	a	b	c	a	b	c
GaN	1.3820	0.4596	0.9079	0.6996	0.4584	1.1533
GaP	2.4437	0.4938	0.8844	1.1731	0.4890	1.1541
GaAs	2.4981	0.4889	0.8762	1.2382	0.4894	1.1484
GaSb	3.0431	0.5153	0.8653	1.4387	0.5095	1.1442
InAs	2.9012	0.5152	0.8632	1.3759	0.5099	1.1418
InSb	3.2265	0.5241	0.8549	1.5213	0.5181	1.1360

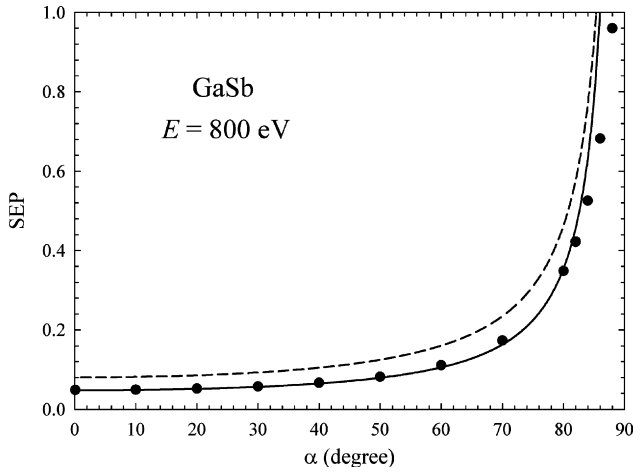

Fig. 3. A plot of the SEP as a function of crossing angle for 800 eV electrons crossing a GaSb surface from vacuum. The solid circles are the results calculated here using Eq. (6), and the solid and dashed curves are the fit results found here using Eq. (8) and previously [36].

Fig. 4 shows a plot of the total SEP (solid circles) calculated using Eqs. (5) and (6) as a function of electron energy for a double crossing, i.e., with a 50° incident angle and a 0° escaping angle for the GaP surface. Fits to these results using Eq. (8) (solid curve) and to previous results [36] (dashed curve) as well as the experimental results of Orosz et al. [37] (open circles) are included for comparisons. It is seen that the SEP decreases with increasing electron energy due to the smaller interaction time between the electron and the surface. The difference between our present and previous results is due to the fact that the laws were only approximately satisfied in our earlier work. The data of Orosz et al. were deduced from experimental inelastic-scattering cross sections extracted from REELS measurements using the method of Tougaard et al. [1,38]. These data contain a contribution from surface excitations by an electron moving both inside and outside the solid [39]. The present work, however, only dealt with the contribution from surface excitations by an electron moving outside the solid. When an electron moves inside the solid, the probability of surface excitations approximately compensates that for the decrease of volume excitations [13]. In other words, as an electron moves away from the surface inside the solid, the decrease in surface excitations is almost the same as the increase in volume excitations. Therefore, the probability of surface excitations for an electron moving inside the solid is treated together with volume excitations. The different treatments result in expected differences of about a factor of two between the results of the present work (solid circles) and those of Orosz et al. (open circles).

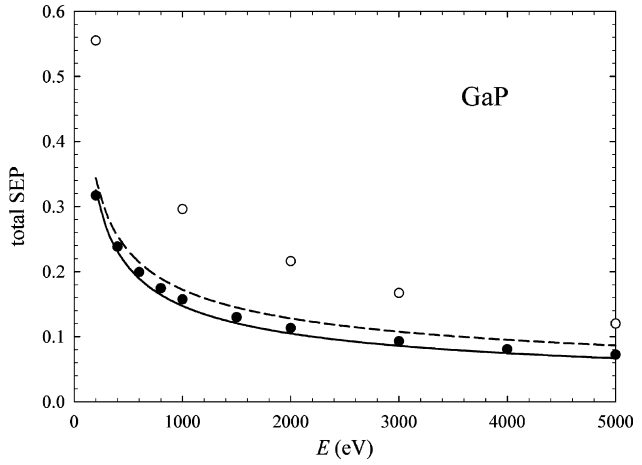

Fig. 4. A plot of the total SEP as a function of electron energy for electrons incident at 50° on a GaP surface escaping at an angle of 0°. The solid circles are results calculated using Eqs. (5) and (6), and the solid and dashed curves are the fit results found here using Eq. (8) and previously [36]. The open circles are the experimental data of Orosz et al. [37].

4. Conclusions

Extended Drude dielectric functions were used to determine the response of GaN, GaP, GaAs, GaSb, InAs and Insb semiconducting III–V compounds to electrons moving across the solid surface. Parameters in the dielectric functions were established from fits to experimental optical data and electron energy-loss spectra. Based on the dielectric response theory, IMFPs for electrons of energies between 200 and 2000 eV were calculated. It was found that the calculated results were in good agreement with experimental data. The angular and energy dependences of the SEP for electrons moving in vacuum and across the surface were also calculated. It showed that the SEP increased with increasing crossing angle or decreasing electron energy. However, the $(\cos\alpha)^{-1}$ angular dependence worked only approximately. Above an appreciable glancing angle, the SEP increased rapidly with crossing angle. Both the IMFP and the SEP were fitted to simple formulas for applications in surface-sensitive electron spectroscopies.

Surface excitations occur when electrons move on both sides of the surface and depend on electron position. When electrons are inside the solid, it is more convenient to combine the treatment of volume and surface excitations together by assuming a spatially non-varying total excitation probability. This assumption is valid due to the approximate compensation of volume and surface excitations at any electron position inside the solid. When electrons are outside the solid, only surface excitations are possible. In this case, the SEP is used to describe the total probability of surface excitations by electrons moving in vacuum. In the present work, we adopted such a simplified treatment by modeling and calculating the spatially non-varying IMFP and the SEP. This treatment was consistent with the approach of our previous works.

Acknowledgement

This research was supported by the National Science Council of the Republic of China under Contract No. NSC94-2215-E-009-080.

References

[1] S. Tougaard, I. Chorkendorff, Phys. Rev. B 35 (1987) 6570.
[2] C.J. Tung, Y.F. Chen, C.M. Kwei, T.L. Chou, Phys. Rev. B 49 (1994) 16684.
[3] Y.F. Chen, P. Su, C.M. Kwei, C.J. Tung, Phys. Rev. B 50 (1994) 17547.
[4] R.H. Ritchie, Phys. Rev. 106 (1957) 874.
[5] G. Chiarello, E. Colavita, M. De Cresenzi, S. Nannarone, Phys. Rev. B 29 (1984) 4878.
[6] Y. Ohno, Phys. Rev. B 39 (1989) 8209.
[7] J.C. Ingham, K.W. Nebesny, J.E. Pemberton, Appl. Surf. Sci. 44 (1990) 279.
[8] F. Yubero, J.M. Sanz, E. Elizalde, L. Galan, Surf. Sci. 237 (1990) 173.
[9] F. Yubero, S. Tougaard, Phys. Rev. B 46 (1992) 2486.
[10] Z.J. Ding, J. Phys.: Condens. Matter 10 (1998) 1733.
[11] M. Vicanek, Surf. Sci. 400 (1999) 1.
[12] Y.F. Chen, C.M. Kwei, Surf. Sci. 364 (1996) 131.
[13] C.M. Kwei, C.Y. Wang, C.J. Tung, Surf. Interface Anal. 26 (1998) 682.
[14] Y.F. Chen, Surf. Sci. 519 (2002) 115.
[15] Y.C. Li, Y.H. Tu, C.M. Kwei, C.J. Tung, Surf. Sci. 589 (2005) 67.
[16] C.M. Kwei, Y.C. Li, C.J. Tung, Surf. Sci. 600 (2006) 3690.
[17] W.S.M. Werner, W. Smekal, H. Störi, Surf. Interface Anal. 31 (2001) 475.
[18] W.S.M. Werner, W. Smekal, C. Tomastik, H. Störi, Surf. Sci. 486 (2001) L461.
[19] W.S.M. Werner, W. Smekal, T. Cabela, C. Eisenmenger-Sittner, H. Störi, J. Elec. Spectroscopy 114–116 (2001) 363.
[20] R. Oswald, Ph. D. Thesis, Eberhard-Karls-Universität, Tübingen, (1992).
[21] C.M. Kwei, Y.F. Chen, C.J. Tung, J.P. Wang, Surf. Sci. 293 (1993) 202.
[22] E.D. Palik (Ed.), Handbook of Optical Constants of Solids, Academic Press, New York, 1985.
[23] E.D. Palik (Ed.), Handbook of Optical Constants of Solids II, Academic Press, New York, 1991.
[24] C.V. Festenberg, Z. Phys. 227 (1969) 453.
[25] G. Brockt, H. Lakner, Micron 31 (2000) 435.
[26] D.Y. Smith, E. Shiles, Phys. Rev. B 17 (1978) 4689.
[27] R.H. Ritchie, A. Howie, Philos. Mag. 36 (1977) 463.
[28] F. Yubero, J.M. Sanz, B. Ramskov, S. Tougaard, Phys. Rev. B 53 (1996) 9719.
[29] Z.J. Ding, J. Phys.: Condens. Matter 10 (1998) 1753.
[30] R.F. Egerton, Electron Energy-Loss Spectroscopy in the Electron Microscope, Plenum, New York, 1986.
[31] C.J. Tung, R.H. Ritchie, Phys. Rev. B 16 (1977) 4302.
[32] C.M. Kwei, L.W. Chen, Surf. Interface Anal. 11 (1988) 60.
[33] G. Gergely, M. Menyhard, S. Gurban, Zs. Benedek, Cs. Daroczi, V. Rakovics, J. Tóth, D. Varga, M. Krawczyk, A. Jablonski, Surf. Interface Anal. 30 (2000) 195.
[34] S. Tanuma, C.J. Powell, D.R. Penn, Surf. Interface Anal. 17 (1991) 911.
[35] W.H. Gries, Surf. Interface Anal. 24 (1996) 38.
[36] C.M. Kwei, Y.H. Tu, C.J. Tung, Nucl. Instrum. Methods B 230 (2005) 125.
[37] G.T. Orosz, G. Gergely, S. Gurban, M. Menyhard, J. Toth, D. Varga, S. Tougaard, Vacuum 71 (2003) 147.
[38] S. Tougaard, J. Kraaer, Phys. Rev. B 43 (1991) 1651.
[39] G. Gergely, M. Menyhard, S. Gurban, A. Sulyok, J. Toth, D. Varga, S. Tougaard, Surf. Interface Anal. 33 (2002) 410.